Fluorescence Intensity Multiple Distributions Analysis: Concurrent Determination of Diffusion Times and Molecular Brightness

Kaupo Palo,* Ülo Mets,* Stefan Jäger,* Peet Kask,*[†] and Karsten Gall*

*EVOTEC BioSystems AG, D-22525 Hamburg, Germany, and [†]Institute of Experimental Biology, Harku 76902, Estonia

ABSTRACT   Fluorescence correlation spectroscopy (FCS) has proven to be a powerful technique with single-molecule sensitivity. Recently, it has found a complement in the form of fluorescence intensity distribution analysis (FIDA). Here we introduce a fluorescence fluctuation method that combines the features of both techniques. It is based on the global analysis of a set of photon count number histograms, recorded with multiple widths of counting time intervals simultaneously. This fluorescence intensity multiple distributions analysis (FIMDA) distinguishes fluorescent species on the basis of both the specific molecular brightness and the translational diffusion time. The combined information, extracted from a single measurement, increases the readout effectively by one dimension and thus breaks the individual limits of FCS and FIDA. In this paper a theory is introduced that describes the dependence of photon count number distributions on diffusion coefficients. The theory is applied to a series of photon count number histograms corresponding to different widths of counting time intervals. Although the ability of the method to determine specific brightness values, diffusion times, and concentrations from mixtures is demonstrated on simulated data, its experimental utilization is shown by the determination of the binding constant of a protein–ligand interaction exemplifying its broad applicability in the life sciences.

INTRODUCTION

Magde et al. (1972) demonstrated the feasibility of detecting molecular number fluctuations by fluorescence correlation spectroscopy (FCS). Since then an increasing number of publications has appeared, aimed at improving the performance and accuracy of this technique. A major progress was the implementation of confocal detection optics (Koppel et al., 1976; Rigler and Widengren, 1990) and the use of silicon photon detectors (Rigler et al., 1993a). This development pushed the detection limit below the single-molecule level (Rigler et al., 1993b; Eigen and Rigler, 1994; Brand et al., 1997; Eggeling et al., 1998). In recent publications covering fluorescence fluctuation spectroscopy the attention has been drawn toward analyzing the histogram of the number of photon counts rather than the autocorrelation function (Qian and Elson, 1990; Fries et al., 1998; Chen et al., 1999; Kask et al., 1999). Whereas fluorescence intensity distribution analysis (FIDA) relies on a collection of instantaneous values of the fluctuating intensity, FCS analyzes the temporal characteristics of the fluctuations. Hence, the two methods represent complementary tools; FCS resolves components with different diffusion coefficients, while FIDA distinguishes the species according to their different values of specific molecular brightness.

In this study we present a method that extracts both characteristics (diffusion time and molecular brightness) from a single measurement, increasing the readout effectively by one dimension. This is achieved by recording the histograms of the number of photon counts using multiple widths of counting time intervals simultaneously. In contrast to other two-dimensional FIDA techniques (Kask et al., 2000), which use two detectors, here only a single detector is needed. The viability of this new method, which we shall call fluorescence intensity multiple distributions analysis (FIMDA), is supported by measurements characterizing a real protein–ligand interaction. The method can be widely applied for monitoring molecular interactions including receptors and ligands or antibodies and antigens, which are both of great relevance in the life sciences.

THEORY

FIDA has been introduced as a method for analyzing mixtures of fluorescent particles. It is based on the detection of instantaneous photon emission rates from an open confocal volume. The central part of the method is the collection of photon count numbers, recorded in time intervals of fixed duration (time windows) and using this information to build up a count number histogram. A theoretical probability distribution of photon count numbers is fitted against the obtained histogram yielding specific brightness values q, and concentrations c, for all different species in the sample. The historic predecessor of FIDA is FCS, which distinguishes different species on the basis of their characteristic diffusion times τ, by analyzing the second-order autocorrelation function of light intensity, $G(t) = \langle I(0)I(t) \rangle - \langle I \rangle^2$. Parameters that can be determined by FCS (in addition to diffusion times τ) are not, however, concentrations and specific brightness values of different species separately, but products of the form cq^2. It is noteworthy that FCS and FIDA are complementary methods that can be applied to analyze the same sequence of photon counts.

The present study is aimed at developing a method that unifies—in a possibly minimal way—the advantages of

both techniques. The key is to analyze a set of distributions that is sensitive to the translational diffusion of particles. FCS detects the dynamics of particles because it compares the instantaneous intensities at time intervals separated by a certain delay. In order to make the distribution of photon count numbers sensitive to the temporal evolution of intensity one may alternatively choose to build a set of photon count number distributions corresponding to different time windows. The choice of the time windows should span a range comparable to the delay values used in FCS.

In the following we will present a modification of the theory of FIDA (Kask et al., 1999), which is a suitable approximation for our experimental purposes. In FIDA, a convenient representation of a photon count number distribution $P(n)$ is its generating function, defined as

$$R_{P(n)}(\xi) = \sum_n \xi^n P(n).$$ (1)

The simple theory of FIDA assumes (1) that molecules are immobile during the counting time interval, and (2) that the light flux from a molecule can be expressed as a product of a spatial brightness function $B(\mathbf{r})$ (this is a function of spatial coordinates of the molecule characterizing the equipment) and a specific brightness q (characterizing a certain molecule species). Under these two assumptions, the distribution of the number of photon counts, emitted by molecules from a volume element dV, is double Poissonian and the corresponding generating function reads

$$R_{P(n)}(\xi) = \exp[cdV(e^{(\xi-1)qB(\mathbf{r})T} - 1)],$$ (2)

where ξ is the complex argument of the generating function, c is the concentration of molecules, and T is the width of the counting time interval. The representation we use is particularly convenient because contributions from independent sources, like different volume elements or species, are combined by simple multiplication of the contributing generating functions. The generating function of $P(n)$ for a single species is

$$R_{P(n)}(\xi) = \exp\left[c\int(e^{(\xi-1)qB(\mathbf{r})T} - 1)dV\right],$$ (3)

while accounting for multiple species simply yields

$$R_{P(n)}(\xi) = \exp\left[\sum_i c_i\int(e^{(\xi-1)q_iB(\mathbf{r})T} - 1)dV\right].$$ (4)

The integral on the right-hand side of Eq. 4 is calculated numerically, but instead of the three-dimensional integration over spatial coordinates, a one-dimensional integration coordinate $x = \ln[B_0/B(\mathbf{r})]$ is introduced. The relationship between the brightness B and the coordinate x is therefore $B(x) = B_0e^{-x}$. In FIDA it is suitable to express the function

dV/dx, which describes the brightness profile in one-dimensional representation, by the formula:

$$\frac{dV}{dx} = A_0(x + a_1x^2 + a_2x^3).$$ (5)

Here a_1 and a_2 are empirical adjustment parameters granting for a sufficient flexibility to fit the measured histograms with high precision. The selection of coefficients A_0 and B_0 is nothing but the selection of the units of V and B. Usually, they are determined from the conditions

$$\int BdV = 1,$$ (6)

$$\int B^2dV = 1.$$ (7)

So far, we have described a simple version of the theory of FIDA. For the purposes of FIMDA, we have to abandon the assumption that molecules are immobile during the counting interval. Surprisingly, we will not abandon Eq. 2, and the following equations, but we will redefine the meaning of some variables instead; x is still a variable related to the spatial brightness profile, but now it characterizes the path of the molecule rather than its position. B is the spatial brightness averaged over the path rather than determined at a fixed position of the molecule. V is not the volume in space but dV/dx still expresses the probability that a molecule has a given value of x. If we would keep the original meaning of c and q, we would have to develop a theory predicting how A_0, a_1, and a_2 depend on the counting time interval T. However, we have chosen another approach. We kept the normalization conditions (Eqs. 6 and 7) and even found it possible to apply a *single* selection of the values A_0, a_1, and a_2 for a set of *different* time windows. The consequence of this selection is that in Eqs. 2–4 c is an apparent concentration (c_{app}) and q is an apparent brightness (q_{app}), which both depend on the width of the counting time interval T.

In the following, a theory is presented predicting how c_{app} and q_{app} depend on T. We will study the case of single species and calculate the first and the second factorial cumulants of the distribution corresponding to Eq. 3. The factorial cumulants are defined as

$$K_n = \left(\frac{\partial}{\partial\xi}\right)^n \ln(R(\xi))|_{\xi=1}$$ (8)

yielding:

$$K_1 = \langle n \rangle = c_{app}q_{app}T,$$ (9)

$$K_2 = \langle n(n-1) \rangle - \langle n \rangle^2 = c_{app}q_{app}^2T^2,$$ (10)

where we have used normalization conditions given by Eqs. 6 and 7. (Note that Eqs. 9 and 10 are in total agreement with Qian and Elson's formulae (1990) derived under assumptions 1 and 2.) From Eq. 9 one can easily conclude that

$$c_{app}(T)q_{app}(T) = \langle I \rangle, \tag{11}$$

where $\langle I \rangle \equiv \langle n \rangle_T/T$ is the mean count rate, which does not depend on the choice of T. We shall proceed by using the following relationship between the second cumulant of the count number distribution $P(n; T)$ and the autocorrelation function of fluorescence intensity $G(t) = \langle I(0)I(t) \rangle - \langle I \rangle^2$,

$$\langle n(n - 1) \rangle_T - \langle n \rangle_T^2 = \int_0^T dt_1 \int_0^T dt_2 G(t_2 - t_1). \tag{12}$$

Introducing the notation

$$\Gamma(T) = \frac{1}{c_{app}(0)q_{app}^2(0)T^2} \int_0^T dt_1 \int_0^T dt_2 G(t_2 - t_1), \tag{13}$$

we get from Eqs. 12 and 10

$$c_{app}(T)q_{app}^2(T) = c_{app}(0)q_{app}^2(0)\Gamma(T). \tag{14}$$

From Eqs. 11 and 14 we get

$$c_{app}(T) = \frac{c_{app}(0)}{\Gamma(T)}, \tag{15}$$

$$q_{app}(T) = q_{app}(0)\Gamma(T). \tag{16}$$

As the concluding step in our present theory, we shall substitute the well-known and tested expressions of $G(t)$ from FCS into Eq. 13. If we ignore triplet trapping and study pure diffusion, then $c_{app}(0)$ is the true concentration c, and $q_{app}(0)$ is the true specific brightness q. Applying a Gaussian brightness function (Aragón and Pecora, 1976), the autocorrelation function is

$$G_{diff}(t) = cq^2 \left(1 + \frac{D|t|}{\sigma_r^2}\right)^{-1} \left(1 + \frac{D|t|}{\sigma_z^2}\right)^{-1/2}, \tag{17}$$

denoting D as the diffusion coefficient and σ_r as the radial and σ_z as the longitudinal distance, where the Gaussian profile has dropped $e^{1/2}$ times. The integrals in Eq. 13 yield the correction factor for translational diffusion

$\Gamma_{diff}(t)$

$$= \frac{4}{t^2\beta\sqrt{1 - \beta}} \left[\beta(1 + t)\text{artanh}\left(\frac{\sqrt{1 - \beta}(\sqrt{1 + \beta t} - 1)}{\beta + \sqrt{1 + \beta t} - 1}\right) - \sqrt{1 - \beta}(\sqrt{1 + \beta t} - 1)\right], \tag{18}$$

where $t = DT/\sigma_r^2$ and $\beta = \sigma_r^2/\sigma_z^2$. For reasons explained below it is useful to calculate the first-order terms in Eq. 18:

$$\Gamma_{diff}(T) = \left[1 + \frac{DT}{6}\left(\frac{2}{\sigma_r^2} + \frac{1}{\sigma_z^2}\right)\right]^{-1} + O(D^2). \tag{19}$$

However, from theoretical considerations and measurements it is known that simple physical models like Gaussian or Gaussian-Lorentzian do not exactly represent the actual brightness profile (Kask et al., 1999). Therefore, we modified Eq. 19 and introduced a fitting parameter a that preserves the first-order terms in Eq. 19:

$$\Gamma_{diff}(T) \approx \left[1 + \frac{DT}{6a}\left(\frac{2}{\sigma_r^2} + \frac{1}{\sigma_z^2}\right)\right]^{-a}. \tag{20}$$

By matching the second-order terms the Gaussian brightness profile would correspond to $a = 2/3$, but we rather choose a to be an empirical parameter, which has to be determined by the fitting procedure. From Eqs. 15 and 16 we can express the apparent parameters of a pure diffusion process:

$$c_{app}^{(diff)}(T) = \frac{c}{\Gamma_{diff}(T)}, \tag{21}$$

$$q_{app}^{(diff)}(T) = q\Gamma_{diff}(T). \tag{22}$$

Another well-known phenomenon involved is that of intensity fluctuations due to trapping of molecules into a triplet excited state (Widengren et al., 1995). To obtain a good fit, particularly at values of T comparable to the triplet lifetime (which is typically 2 μs), an additional factor has to be introduced into $G(t)$:

$$F_{trip}(t) = \frac{1 + \kappa\tau \exp\left(-\frac{(1 + \kappa\tau)|t|}{\tau}\right)}{(1 + \kappa\tau)^2}, \tag{23}$$

where κ is the singlet to triplet transition rate and τ is the triplet lifetime. As the following step we may consider Eq. 23 with an additional factor of cq^2 as a correlation function of an ensemble of immobile particles undergoing triplet transitions:

$$G_{trip}(t) = cq^2 F_{trip}(t) \tag{24}$$

From Eq. 13 and 24 we can compute

$\Gamma_{trip}(T)$

$$= \frac{\left\{2\frac{\tau}{T}\kappa\tau\left[1 + \kappa\tau - \frac{\tau}{T}(1 - e^{-(T/\tau)(1 + \kappa\tau)})\right] + (1 + \kappa\tau)^2\right\}}{(1 + \kappa\tau)^3}. \tag{25}$$

Unlike diffusion, which influences only higher cumulants of photon count numbers, triplet corrections also shift the first cumulant by the factor $1/(1 + \kappa\tau)$.

$$c_{\text{app}}^{(\text{trip})}(T)q_{\text{app}}^{(\text{trip})}(T) = \frac{cq}{1 + \kappa\tau},$$

$$c_{\text{app}}^{(\text{trip})}(T)q_{\text{app}}^{(\text{trip})}(T)^2 = \frac{cq^2\Gamma_{\text{trip}}(T)}{1 + \kappa\tau}. \tag{26}$$

Solving these equations with respect to $q_{\text{app}}^{(\text{trip})}$ and $c_{\text{app}}^{(\text{trip})}$ yields

$$c_{\text{app}}^{(\text{trip})}(T) = \frac{c}{\Gamma_{\text{trip}}(T)(1 + \kappa\tau)}, \tag{27}$$

$$q_{\text{app}}^{(\text{trip})}(T) = q\Gamma_{\text{trip}}(T). \tag{28}$$

Now, having solved the problems with diffusion and triplet transitions separately, we shall study the joint problem. Usually, the time scale of triplet transitions is much shorter than that of diffusion. Therefore, we are justified to replace c and q in Eqs. 21 and 22 by $c_{\text{app}}^{(\text{diff})}$ and $q_{\text{app}}^{(\text{diff})}$. This lets us combine Eqs. 21, 22, 27, and 28 to express c_{app} and q_{app} as

$$c_{\text{app}}(T) = \frac{c}{\Gamma_{\text{trip}}(T)\Gamma_{\text{diff}}(T)(1 + \kappa\tau)}, \tag{29}$$

$$q_{\text{app}}(T) = q\Gamma_{\text{trip}}(T)\Gamma_{\text{diff}}(T).$$

After having derived these expressions for c_{app} and q_{app}, the data simulations and the experiments should verify their validity.

MATERIALS AND METHODS

Experimental set-up

The central optical part of a FIMDA experiment is a confocal microscope as it is used in fluorescence correlation spectroscopy (Koppel et al., 1976; Rigler et al., 1993a). For the excitation of fluorescence, a beam from a continuous wave laser is attenuated to ~800 μW by neutral density filters, passes a beam expander, and is directed to the microscope objective (UApo/340, 40×, N.A. 1.15, Olympus Optical Co. Ltd., Tokyo, Japan) by a dichroic mirror. Fluorescence is collected by the same objective through the dichroic mirror, a spectral band-pass filter, and is focused to a confocal pinhole, which serves to reject the out-of-focus light. The light, which passes the pinhole, is detected by a silicon photon counting module (SPCM-AQ-131, EG&G Optoelectronics, Vaudreuil, Canada). An electronic counter, constructed at EVOTEC as a computer plug-in card, collects the TTL pulses from the detector continuously and calculates the count number histograms for all preselected widths of time windows (40, 60, 120, 200, 400, 600, 800, 1200, 1600, 2000 μs) in real time from the 32 MB onboard buffer. By feeding the detector outputs to a correlator, FCS measurements can be performed in parallel with FIMDA experiments.

In order to satisfy the spectral needs of the various fluorophores used in this study, different lasers and spectral band-pass filters were employed. For Cy5 (Amersham Pharmacia Biotech, Bucks, UK) conjugated biomolecules an arrangement of a red laser diode (Crystal GmbH, Berlin, Germany; 635 nm) and a band-pass filter with a central wavelength of 670 nm

(670DF40, Omega Optical, Brattleboro, VT) was used. In case of TAMRA (5-carboxytetramethylrhodamine) labeled molecules this was an arrangement of a frequency doubled Nd-YAG laser (μGreen 4601; Uniphase, San Jose, CA; 532 nm) and a 590DF60 filter.

The effective dimensions of the illuminated volume were calibrated indirectly, using FCS on small dye molecules (TAMRA, Cy5) with known diffusion coefficients. The autocorrelation functions of diffusion were fitted to Eq. 17, i.e., assuming a three-dimensional Gaussian intensity profile. The exact determination of the dimensions and profile would be very complex because they are affected by both the size of the laser beam and the size of the confocal pinhole. However, in most cases the knowledge of the exact dimensions is not necessary.

The focal beam radius was adjusted to ~0.75 μm by selecting an appropriate expansion factor of the original laser beam, resulting in a mean translational diffusion time of 360 μs for the free dye Cy5. This diffusion can be clearly observed when raising the time windows from 40 μs to 2 ms. As can be seen in Fig. 1, the selected count number distributions of a 3.8 nM Cy5 solution differ considerably. However, the major differences between the distributions are due to the varying mean count number in different time windows used. Diffusion of fluorescent molecules causes only small but significant modifications to the shape of each distribution.

The levels of background count rate are determined in a separate experiment on bidistilled water and amount usually to 0.5 kHz. The main contributor to this non-fluctuating background light intensity is Raman scattering from water.

Data simulations

Real samples, comprising a mixture of molecules, which express deliberately chosen parameters (brightness values and diffusion coefficients), are difficult to prepare. Therefore, some evaluations of the new method were performed using simulated data. A number of sets of histograms for FIMDA, FIDA, and correlation functions for FCS have been simulated according to the following algorithm. In a closed rectangular reservoir, a given number of molecules is initially randomly distributed over a high number (typically 360 × 360 × 720) of discrete spatial grid points. Each molecule is subject to consequent diffusion simulation and jumps randomly by one grid unit either in an x-, y-, or z-direction with a frequency corresponding to a given diffusion coefficient. The "focus" is located in the center of the reservoir, and the brightness distribution is assumed to be Gaussian in all three dimensions. When calculating the brightness integral from a molecule over a given set of time intervals, the molecule can be randomly trapped and released from the triplet excited state (where it is dark). Now we can calculate an array of brightness integrals over basic time intervals of a given width (e.g., 5 μs) describing the evolution of the mixture. The brightness integrals are then converted into photon count numbers by generating a random Poisson number with the corresponding average. This step also accounts for the noise introduced by the detector because the random number generator is used not only for driving random motion of molecules but also for simulating random numbers of detected photons at given light intensities. The random count numbers obtained were subsequently used to calculate histograms for FIMDA, FIDA, and the correlation function for FCS.

Due to the finite size of the simulation reservoir, some distortions of the correlation function (i.e., deviations from Eq. 17) can be expected. The distortions are in fact below the statistical noise level. Therefore we consider the simulations to be an adequate tool for estimating statistical errors of the extracted parameters. For this purpose, typically 30 realizations of experiments with a given set of molecular parameters were simulated, from which the standard deviations and the coefficients of variation (CV) as the ratio of standard deviation to mean value were calculated.

Fitting

A series of simultaneously measured or simulated distributions is globally fitted using a Marquardt algorithm. The fitting program is a modest modification of the program designed for FIDA (Kask et al., 1999). Theoretical distributions are calculated using exactly the same algorithm as in FIDA, except that each species has an individual apparent concentration and an apparent brightness at each time window, calculated according to Eqs. 29. All parameters not assigned to species but rather to the equipment (i.e., A_0, a_1, and a_2 from Eq. 5 and a from Eq. 20) are usually determined beforehand from separate adjustment experiments on pure dye solutions.

Biochemical system

The Grb2 (SH2)-phosphopeptide interaction

Recent antitumor research has been focused on tyrosine kinase growth factor receptors (Levitzki, 1994; Alessandro et al., 1996; Furet et al., 1998). A critical link in the signal transduction pathway of this receptor is the interaction of its phosphotyrosine residue (pTyr) with the Src-homology 2 (SH2) domain of the adapter protein Grb2 (growth factor receptor-binding protein 2). For the recognition, a minimal peptide sequence of the receptor (pTyr-Val-Asn) is sufficient (Müller et al., 1996; Gram et al., 1997; Furet et al., 1998). The binding partner of this peptide motive, the SH2 domain of Grb2, can fold into a functional protein module independent of neighboring sequences (Booker et al., 1992; Overduin et al., 1992). Therefore, as a model system, we have chosen the bare SH2 domain (14.3 kDa) to interact with a fluorescently labeled phosphopeptide (pTyr-Val-Asn-Val-Lys(Cy5)) (1387 Da).

The SH2 domain of Grb2 was prepared as described elsewhere (Lowenstein et al., 1992; Baumann et al., 1994; Müller et al., 1996). The phosphopeptide was synthesized using manual Fmoc solid phase chemistry and labeled with Cy5-NHS via a lysine residue. An additional valine was introduced to minimize possible interactions of the dye with the main recognition motive pTyr. The final compound, pTyr-Val-Asn-Val-Lys(Cy5), was characterized by mass spectrometry (LC/MS, and MALDI/TOF), UV/VIS, and fluorescence spectroscopy.

RESULTS

Data simulations and test experiments

At first, a series of measurements on a 1 nM TAMRA solution was performed collecting data in parallel for FIMDA and FCS. This series of experiments, with duration of 2 s each, was repeated in simulations using similar molecular parameters. The purpose of these experiments was to verify whether simulations are a reasonable model of real experiments, in particular whether data simulations are a reasonable means of predicting statistical errors of estimated parameters. The coefficients of variation of the parameters extracted from simulated data indeed coincide with the results of the real experiment, as can be seen in Table 1.

Another series of test experiments was repeated in a significantly shorter time domain with the goal of comparing FIMDA and FCS in their ability to estimate parameters of the triplet component. A set of counting time intervals of 2, 4, 8, 16, 32, 64, 128, 256, 512, and 1024 μs was selected for this purpose. The duration of these experiments was 16 s. The results, presented in Table 2, indicate that the values for the triplet parameters estimated by FIMDA have
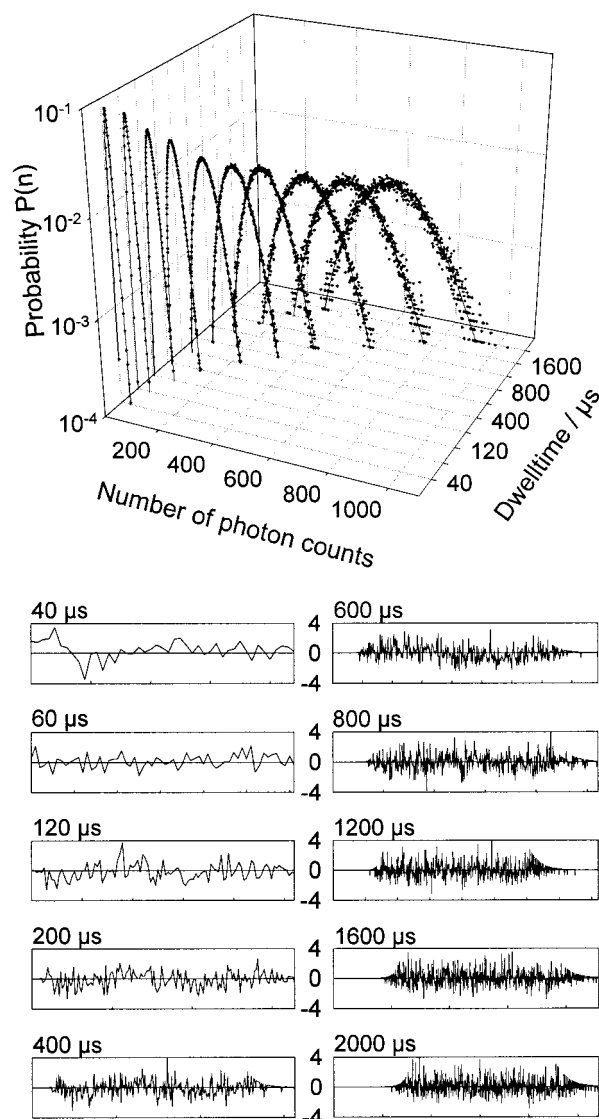

FIGURE 1 Count number distributions and fits of a 3.8 nM Cy5 solution recorded simultaneously at different time windows T. The weighted residuals for the different time windows are shown in the lower part of the figure.

similar dependence on the excitation intensity to the FCS results. It is not surprising that the FIMDA results are slightly biased and have higher CV values compared to FCS, since the estimation of triplet parameters in FIMDA is indirect, because the shortest time window (2 μs) is equal to the triplet lifetime. However, the main purpose of the triplet correction in the model is not to determine the triplet parameters, but to improve the quality of the fit and to remove a source of bias in the brightness and diffusion parameters. The bias in the estimated triplet parameters as presented in Table 2 disappears when introducing corrections for the dead time of the detector.

Out of curiosity, we also simulated histograms for FIMDA for three-component analysis. Two of the compo-

TABLE 1 Comparison of coefficients of variation of estimated parameters from series of experimental and simulated histograms by FIMDA, and correlation functions by FCS

| | | CV (%) | | | |
| | | FIMDA | | FCS | |
Parameter	Mean Value	Experimental Data	Simulated Data	Experimental Data	Simulated Data
Brightness q (kHz)	115	2.5	2.3	2.6	2.5
Concentration c (molecules per confocal volume)	0.73	3.1	3.8	3.8	4.0
Diffusion time τ (μs)	287	5.4	4.3	7.3	5.2

The diffusion time τ is defined as $\tau = G_r^2/D$, whereas the axis ratio G_z/G_r has been fixed to 3.0 (compare Eqs. 17–20).

nents had equal brightness values (120 kHz), and another pair had equal diffusion times (192 μs). Due to the larger number of free parameters, the simulated duration of experiments was increased to 60 s, so that the variations of fitted parameters stayed within reasonable limits. In this test, all parameters were subject to fitting. The results are presented in Fig. 2 as vertical bars in a plane with brightness and diffusion time as *x-y* coordinates, and the ordinate displaying the contribution to the intensity, i.e., the product of concentration and brightness. It is obvious that the three components are clearly resolved, because the scatter in the location of individual bars is much smaller than the distance between the groups, which correspond to different components.

Note that with FIDA alone the components with equal brightness cannot be resolved; with FCS alone, the components with equal diffusion time remain unresolved.

Biochemical system

The experimental utilization of the new method will be demonstrated by the determination of the binding constant of the above-introduced Grb2 (SH2)-phosphopeptide interaction. For this purpose a titration experiment was carried out, keeping the pTyr-Val-Asn-Val-Lys(Cy5) concentration constant at 0.4 nM, while SH2 was subject to titration (0.01, 0.03, 0.1, 0.3, 1, 3, 10, 30, 100, and 130 μM). All experiments were performed under identical conditions, i.e., the same buffer (sterile filtered water, 50 mM sodium phosphate buffer pH 7.8, 50 mM NaCl, and 0.05% Pluronic; $T = 20°C$), and a data acquisition time of 30 s per measurement,

repeated 30 times per sample. In each single measurement the same set of 10 different time windows was used (40, 60, 120, 200, 400, 600, 800, 1200, 1600, 2000 μs) resulting in 10 different photon count number histograms, which were globally fitted.

As the first step, the diffusion time $\tau_1 = 407 \pm 6$ μs and the molecular brightness $q_1 = 31.7 \pm 0.3$ kHz were determined from a single component analysis applied to the pure conjugate solution. Addition of excess SH2 (130 μM) to 0.4 nM conjugate resulted in a sample with the majority of the conjugate bound to SH2. The complex was characterized both by a longer diffusion time and a higher molecular brightness compared to the free conjugate. This mixture was then analyzed by all three methods (FIMDA, FIDA, and FCS) using a two-component fit with τ_1 and/or q_1 fixed, depending on the method. The results of this step of analysis are presented in Table 3. It can be seen that all methods yield similar values of parameters for the complex. The corresponding CV values were again determined by two independent methods, i.e., from the statistical analysis of the results of a series of 30 measurements and from simulations. The two estimates of the statistical errors agree reasonably well and the CV values corresponding to different methods are similar, with the exception of FIDA, which has difficulties due to the small (30%) difference in specific brightness of the two components.

As the next step of our studies, a sample with 3 μM SH2 was analyzed. This particular concentration was chosen to achieve a mixture of approximately equal proportions of complex and free conjugate. Because it is rather difficult to resolve components with only a twofold difference in dif-

TABLE 2 Triplet parameters estimated from a series of experiments on 1 nM TAMRA solution by FCS and FIMDA at two different excitation intensities. Excitation wavelength 532 nm, duration 16 s, time windows 2, 4, 8, 16, 32, 64, 128, 256, 512, and 1024 μs

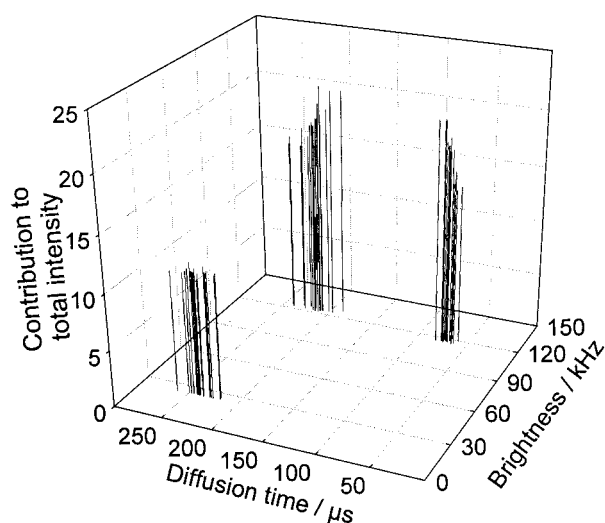| Peak Excitation Intensity (kW/cm^2) | FCS | | | | FIMDA | | | |
	Triplet Lifetime (μs)	CV (%)	Triplet Population	CV (%)	Triplet Lifetime (μs)	CV (%)	Triplet Population	CV (%)
118	1.98	3.9	0.182	2.7	3.12	7.6	0.137	3.1
187	1.75	3.7	0.235	1.6	2.59	3.8	0.183	2.0

FIGURE 2 Fitting results of simulated data for a mixture of three components. The simulated brightness (in kHz) and diffusion time (in μs) values for the components are 30 kHz, 192 μs; 120 kHz, 192 μs; 120 kHz, 64 μs. The contributions to the total intensity are 10.8, 20.4, and 14.4, respectively. The graph presents the results of FIMDA from 20 independent realizations of simulations, each corresponding to an experiment of 60 s duration.

fusion coefficient and even smaller difference in specific brightness, here also the diffusion time and brightness of the complex were fixed to the values of Table 3. With the molecular parameters fixed, the concentrations were reliably determined by all methods. The results of this step of analysis are summarized in Table 4.

In the same manner, the whole series of SH2 concentrations was fitted. Figure 3 shows the calculated fraction bound ($c_{\text{complex}}/(c_{\text{complex}} + c_{\text{conjugate}})$) for FIMDA with the

solid curve resulting from a hyperbolic fit that yielded a binding constant for the SH2-phosphopeptide interaction of $K_{\text{D}} = 1.54 \pm 0.14$ μM. Comparable binding curves were also obtained by FCS and FIDA (data not shown), with K_{D} values of 2.16 $\pm$ 0.19 μM and 1.60 $\pm$ 0.19 μM, respectively.

DISCUSSION

The data of Fig. 3 demonstrate that FIMDA is a suitable method for monitoring the formation of a molecular complex. FCS and FIDA experiments yielded similar K_{D} values for this particular SH2-phosphopeptide interaction. In the literature the affinity is reported to vary by several orders of magnitude, depending on the peptide sequence (Müller et al., 1996; Gram et al., 1997; Furet et al., 1998). High affinities are in the range of $K_{\text{D}} = 10 - 100$ nM. However, with a lysine (and Cy5 attached to it) at the +4 position of the phosphopeptide (defining p-Thr as the 0 position with "+" continuing on the C and "−" on the N-terminus) the affinity decreases to the micromolar range. This result agrees well with the importance of lipophilic groups attached to "appropriate" positions on the C-terminus, increasing the binding constant to the SH2-domain (Furet et al., 1998). For example, Val (at position pTyr+3) is making van der Waals contact with a large hydrophobic area on the SH2-domain.

One of the surprising results of this study is that in each of the experiments, the statistical accuracy of the diffusion time estimated by FIMDA is as good as or even better than that estimated by FCS. This is a counter-intuitive result because FCS is directly focused on fitting a diffusion-dependent correlation function $G(t)$, while in FIMDA the

TABLE 3   Comparison of estimated parameters and their coefficients of variation at a high receptor concentration (130 μM). A series of 30 experiments of 30 s duration each was evaluated by FIMDA, FIDA, and FCS. Brightness (in FIMDA and FIDA) and diffusion time (in FIMDA and FCS) of the free conjugate were independently determined and fixed to 31.7 kHz and 407 μs, respectively, in this analysis

Parameter	Method	Mean Value from Experiment	CV (%)	CV (%) from Simulations
$c_{\text{conjugate}}$ (molecules per confocal volume)	FIMDA	0.132*	43*	82*
	FIDA	0.196*	76*	71*
	FCS	0.052*	99*	120*
c_{complex} (molecules per confocal volume)	FIMDA	0.618	9.6	8.0
	FIDA	0.555	26.7	14.9
	FCS	0.710	7.9	12.6
q_{complex} (kHz)	FIMDA	39.5	2.2	2.3
	FIDA	38.4	5.5	3.9
	FCS	36.4	3.7	3.4
τ_{complex} (ms)	FIMDA	0.913	6.9	4.6
	FCS	0.898	5.4	7.2

*Of 30 realizations, in 5 to 10 cases zero conjugate concentration was yielded by the fitting program (negative values are disallowed). This indicates that in this particular example the conjugate concentration could not be properly determined. However, for further data analysis only q_{complex} and τ_{complex} are needed.

TABLE 4 Comparison of the estimated concentrations at an intermediate receptor concentration (3 μM). In addition to the brightness and the diffusion time of the free conjugate, the brightness and/or the diffusion time of the complex were fixed here to values shown in Table 3

Parameter	Method	Mean Value from Experiment	CV (%)	CV (%) from Simulations
$c_{conjugate}$ (molecules per confocal volume)	FIMDA	0.328	11.7	4.9
	FIDA	0.311	16.1	4.9
	FCS	0.303	8.4	8.0
$c_{complex}$ (molecules per confocal volume)	FIMDA	0.437	8.2	3.4
	FIDA	0.455	10.0	3.7
	FCS	0.467	7.8	8.8

diffusion time is estimated only indirectly, namely through the dependence of the apparent brightness on the width of the time window.

A further observation in this respect is that the CV values of the diffusion times are in general higher than those for the brightness values. This also holds true for the theoretical simulations and therefore reflects an effect rooting in the measuring principle. The phenomenon can be explained qualitatively by the different ways these quantities are determined. For simplicity, one may imagine an observation volume with a constant brightness profile $B(\mathbf{r})$ inside. In this case, one only needs to measure the average count rate of a molecule that enters the volume to determine its specific brightness. This requires the detection of many photons per given time interval but can in principle be achieved from a single passage. However, for estimating the diffusion time, one has to determine the mean duration of the diffusion-driven passage, which inevitably requires averaging over many events, even though many photons may be detected each time. Therefore, in an experiment of fixed duration, the specific brightness of a molecule can in principle be determined with a higher accuracy than its diffusion time.

The advantage of FIMDA and its predecessor FIDA over FCS is that both methods yield genuine concentrations of components in the sample, instead of the products of concentration and brightness squared in FCS. Only the independent determination of at least one of the two molecular brightness values enables FCS to determine two concentrations unambiguously, as it was done in the examples above. However, inexperienced users of FCS often silently assume equal molecular brightness when resolving two components. This assumption can cause significantly biased results. FIDA and FIMDA bring this issue to the focus of analysis.

Another advantage of the presented method is its versatility. If FCS or FIDA fail to detect a particular readout upon a biochemical reaction, FIMDA might be able to succeed. The biochemical reaction is not necessarily limited to the binding of two components, but can be any chemical reaction of interest. Using only one detector for recording two physical characteristics in a single measurement makes FIMDA a very efficient method of analysis, which saves precious assay development time.

After the realization of FIDA (Kask et al., 1999) and the presentation of 2D-FIDA (Kask et al., 2000) FIMDA is already the second FIDA-based fluorescence fluctuation method introduced within a short period of time. This demonstrates the high potential of FIDA for being combined with other methods in order to resolve different fluorescent species on the basis of two or more specific physical quantities (like the molecular brightness and the diffusion time in FIMDA). Single-molecule sensitivity and high reliability of two-dimensional analysis make this class of methods really attractive for various applications.
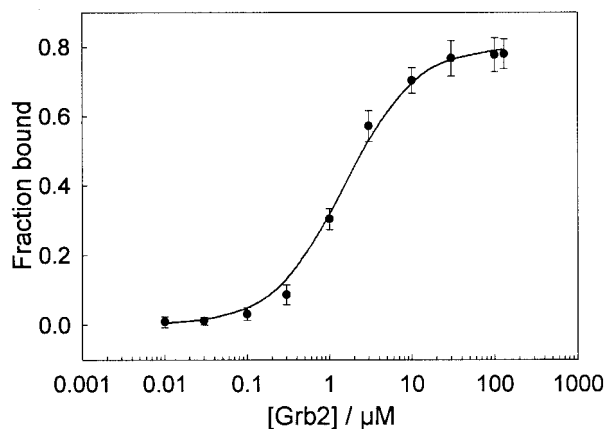
FIGURE 3 Binding of pTyr-Val-Asn-Val-Lys(Cy5) to SH2. The solid curve results from a hyperbolic fit, yielding a binding constant of $K_D = 1.54 \pm 0.14$ μM.

REFERENCES

Alessandro, R., J. Spoonster, R. P. Wersto, and E. C. Kohn. 1996. Signal transduction as a therapeutic target. *Curr. Top. Microbiol. Immunol.* 213:167–188.

Aragón, S. R., and R. Pecora. 1976. Fluorescence correlation spectroscopy as a probe of molecular dynamics. *J. Chem. Phys.* 64:1791–1803.

Baumann, G., D. Maier, F. Freuler, C. Tschopp, K. Baudisch, and J. Wienands. 1994. In vitro characterization of major ligands for Src homology 2 domains derived from protein tyrosine kinases, from the adaptor protein SHC and from GTPase-activating protein in Ramos B cells. *Eur. J. Immunol.* 24:1799–1807.

Booker, G. W., A. L. Breeze, A. K. Downing, G. Panayotou, I. Gout, M. D. Waterfield, and I. D. Campbell. 1992. Structure of an SH2 domain of the p85 alpha subunit of phosphatidylinositol-3-OH kinase. *Nature.* 358:684–687.

Brand, L., C. Eggeling, C. Zander, K. H. Drexhage, and C. A. M. Seidel. 1997. Single-molecule identification of coumarin-120 by time-resolved fluorescence detection: comparison of one- and two-photon excitation in solution. *J. Phys. Chem.* 101:4313–4321.

Chen, Y., J. D. Müller, P. T. So, and E. Gratton. 1999. The photon counting histogram in fluorescence fluctuation spectroscopy. *Biophys. J.* 77:553–567.

Eggeling, C., J. R. Fries, L. Brand, R. Günther, and C. A. Seidel. 1998. Monitoring conformational dynamics of a single molecule by selective fluorescence spectroscopy. *Proc. Natl. Acad. Sci. USA.* 95:1556–1561.

Eigen, M., and R. Rigler. 1994. Sorting single molecules: application to diagnostics and evolutionary biotechnology. *Proc. Natl. Acad. Sci. USA.* 91:5740–5747.

Fries, J. R., L. Brand, C. Eggeling, M. Kollner, and C. A. M. Seidel. 1998. Quantitative identification of different single molecules by selective time-resolved confocal fluorescence spectroscopy. *J. Phys. Chem.* 102:6601–6613.

Furet, P., B. Gay, G. Caravatti, C. Garciaecheverria, J. Rahuel, J. Schoepfer, and H. Fretz. 1998. Structure-based design and synthesis of high affinity tripeptide ligands of the Grb2-SH2 domain. *J. Med. Chem.* 41:3442–3449.

Gram, H., R. Schmitz, J. F. Zuber, and G. Baumann. 1997. Identification of phosphopeptide ligands for the Src-homology 2 (SH2) domain of Grb2 by phage display. *Eur. J. Biochem.* 246:633–637.

Kask, P., K. Palo, N. Fay, L. Brand, Ü. Mets, D. Ullmann, J. Jungmann, J. Pschorr, and K. Gall. 2000. Two-dimensional fluorescence intensity distribution analysis: theory and applications. *Biophys. J.* 78:1703–1713.

Kask, P., K. Palo, D. Ullmann, and K. Gall. 1999. Fluorescence-intensity distribution analysis and its application in biomolecular detection technology. *Proc. Natl. Acad. Sci. USA.* 96:13756–13761.

Koppel, D. E., D. Axelrod, J. Schlessinger, E. L. Elson, and W. W. Webb. 1976. Dynamics of fluorescence marker concentration as a probe of mobility. *Biophys. J.* 16:1315–1329.

Levitzki, A. 1994. Signal-transduction therapy. A novel approach to disease management. *Eur. J. Biochem.* 226:1–13.

Lowenstein, E. J., R. J. Daly, A. G. Batzer, W. Li, B. Margolis, R. Lammers, A. Ullrich, E. Y. Skolnik, S. D. Bar, and J. Schlessinger. 1992. The SH2 and SH3 domain containing protein GRB2 links receptor tyrosine kinases to ras signaling. *Cell.* 70:431–442.

Magde, D., E. L. Elson, and W. W. Webb. 1972. Thermodynamic fluctuations in a reacting system-measurement by fluorescence correlation spectroscopy. *Phys. Rev. Lett.* 29:704–708.

Müller, K., F. O. Gombert, U. Manning, F. Grossmuller, P. Graff, H. Zaegel, J. F. Zuber, F. Freuler, C. Tschopp, and G. Baumann. 1996. Rapid identification of phosphopeptide ligands for SH2 domains: screening of peptide libraries by fluorescence-activated bead sorting. *J. Biol. Chem.* 271:16500–16505.

Overduin, M., C. B. Rios, B. J. Mayer, D. Baltimore, and D. Cowburn. 1992. Three-dimensional solution structure of the src homology 2 domain of c-abl. *Cell.* 70:697–704.

Qian, H., and E. L. Elson. 1990. On the analysis of high order moments of fluorescence fluctuations. *Biophys. J.* 57:375–380.

Rigler, R., and J. Widengren. 1990. Ultrasensitive detection of single molecules by fluorescence correlation spectroscopy. *BioScience.* 40:180–183.

Rigler, R., Ü. Mets, J. Widengren, and P. Kask. 1993a. Fluorescence correlation spectroscopy with high count rate and low background: analysis of translational diffusion. *Eur. Biophys. J.* 22:169–175.

Rigler, R., J. Widengren, and Ü. Mets. 1993b. Interactions and kinetics of single molecules as observed by fluorescence correlation spectroscopy. *In* Fluorescence Spectroscopy: New Methods and Applications. O. S. Wolfbeis, editor. Springer, Berlin. 13–24.

Widengren, J., Ü. Mets, and R. Rigler. 1995. Fluorescence correlation spectroscopy of triplet states in solution: a theoretical and experimental study. *J. Phys. Chem.* 99:13368–13379.